Joint 3D of muon tomography and gravity data to recover density

Kristofer Davis
UBC-Geophysical Inversion Facility
Dept. of Ocean and Earth Sciences
University of British Columbia
6449 Stores Rd
Vancouver, BC V6T 1Z4, Canada
kdavis@eos.ubc.ca

Douglas W. Oldenburg
UBC-Geophysical Inversion Facility
Dept. of Ocean and Earth Sciences
University of British Columbia
6449 Stores Rd
Vancouver, BC V6T 1Z4, Canada
doug@eos.ubc.ca

SUMMARY

Cosmic rays producing muons shower the Earth daily. These natural, high-energy particles decay as they pass through matter and are directly affected by density. Recently, sensors have been placed in existing tunnels and mine shafts that observe muon flux in a brown-field mining scenario. We have developed an algorithm to invert these data individually, or jointly with gravity data, to recover a 3D distribution of density. Muon and gravity data are both linear functionals of density but the associated sensitivity functions are substantially different. These differences in physics between muon ray paths and gravity data provide a unique insight into the subsurface. This is illustrated through synthetic examples. Inversion of a set of field data, obtained at a mine site in south-west British Columbia, Canada, illustrates the potential benefits and challenges for the technique to be used in field surveys.

Key words: muon tomography, joint inversion, gravity, density

INTRODUCTION

Cosmic rays penetrate the upper atmosphere and create pions, which then decay to muons. The muons travel in approximately straight ray paths and the flux is attenuated by the matter passed through. Sensors have been developed to measure the angular distribution of the muon flux underground and the flux information is related to the mass distribution above the detector.

An early application of muon radiography involved searching for hidden chambers in pyramids on the Giza Plateau outside of Cairo, Egypt (Alvarez *et al.,* 1970). Recent application has focussed on the detection of high-density fissile material in containers (e.g. Priedhorsky *et al.,* 2003; Schultz *et al.,* 2004; Wang *et al.,* 2009) and measurements on the magma chambers of volcanoes (e.g. Tanaka *et al* 2010). The motivation of this paper stems from the current collection of muon data in geophysical applications (e.g. Bryman, 2011; Davis *et al.*, 2011). Sensors have been deployed for the re-evaluation of models associated with established deposits (i.e. brown-field scenarios). Detectors are placed at depths below and near the deposit (see Figure 1a for illustration) in existing tunnels. The key advantage of muon data is that they are directly related to the density along a straight ray from the surface to the detector. Muon data therefore have more localized information about the density than do usual gravity data but an inversion is still required.

In this paper we outline the basics of the muon density survey and develop an inversion algorithm. As with any geophysical technique, additional information can greatly reduce inherent non-uniqueness and we illustrate this by jointly inverting the muon data with conventional gravity data. Muons and gravity data are both linear functionals of density but the associated sensitivity functions are substantially different. The two data sets provide complementary information. A synthetic example illustrates the different types of data and the recovered model of density. Data from a field example are inverted and we also discuss practicalities of the field survey.

MUON TOMOGRAPHY

Sensors observe the muon flux as a function of angle over a period of time. The length of time needed for measurements increases with sensor depth because the muon flux is attenuated exponentially with depth. The data are then processed to an integrated path length as a function of a ray-path vector. Angles are binned approximately every 5º within two principal angles: the dip and azimuth (θ and φ, respectively) as shown in Figure 1b. The geometric length is the distance from the surface to the detector at these two angles in space. These processed data are directly related to the amount of mass along the ray path. The i^{th} datum, d_i, is then a function of the i^{th} ray's true geometric length, P_l^i, from the surface and the density, ρ, throughout that path such that

$$d_i = \int_{P_l^i} \rho(l) dl. \qquad (1)$$

In our mathematical representation the earth volume has an upper surface that is determined by the topography and extends deep and wide enough to encompass all ray paths. This volume is discretized into m prismatic cells with constant density. The density becomes a function of three-dimensional space via a vector $\boldsymbol{\rho} = (\rho_1 \ldots \rho_m)^T$. Equation 1 is discretized as

$$d_i = \sum_{j=1}^{m} \mathbf{G}_{ij} \rho_j, \qquad (2)$$

where $\mathbf{G}_{ij}$ is the geometric length of the i^{th} ray path through the j^{th} volume with the density ρ_j and the data have units of m·g/cm^3. The coefficient matrix $\mathbf{G}$ is often referred to the sensitivity matrix. Equation 2 is expressed in vector notation as

$$\mathbf{d}^{tot} = \mathbf{G}\boldsymbol{\rho}. \quad (3)$$

In gravity, the subsurface, ρ, is often thought of as a combination of the background, ρ_b, and anomalous density, Δρ

$$\rho = \rho_b + \Delta\rho\,. \quad (4)$$

The same holds true for muon data. One can assume the background density from prior information (i.e. geology). Equation 3 can be expanded for the muon tomography problem to

$$\mathbf{d}^{tot} = \mathbf{G}\boldsymbol{\rho}_b + \mathbf{G}\Delta\boldsymbol{\rho}\,, \quad (5)$$

and if Δρ is recovered through inversion, the subsurface density can easily be calculated. Therefore, we choose to focus on developing the methodology using density contrast for consistency. The corresponding data are considered anomalous data:

$$\mathbf{d}_a = \mathbf{G}\Delta\boldsymbol{\rho}. \quad (6)$$

As previously discussed, the muon data can be informative by themselves but jointly inverting traditional gravity along with the muon data should yield improved results. Therefore, we now turn to the gravity method to solve for density contrast.

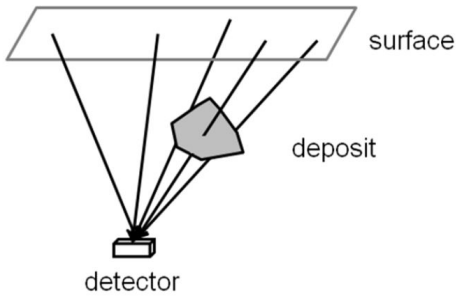

(a)

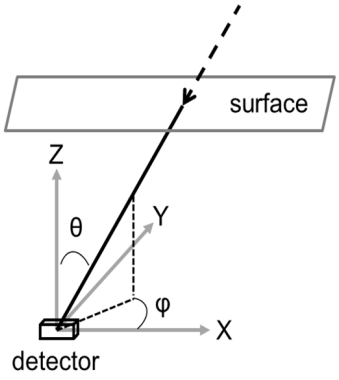

(b)

Figure 1. (a) An illustration showing muon rays from varying angles reaching the detector. A deposit with a high density contrast will cause a smaller muon flux (due to attenuation) than the surrounding geology. (b) The definitions of the angles at which a ray comes from the surface to the detector.

GRAVITY DATA

Gravity data has been studied extensively in the literature so it is only briefly mentioned here. The vertical gravity for the i^{th} datum at location $\mathbf{r}_i$ is

$$d(\mathbf{r}_i) = \gamma \int_V \frac{z - z_i}{|\mathbf{r} - \mathbf{r}_i|^3} \Delta\rho(\mathbf{r}) dV\,, \quad (7)$$

for density $\rho(\mathbf{r})$ throughout volume V (Blakely, 1996; Li and Oldenburg 1998). The density is discretized into the same prismatic volumes as the muon ray paths. The discretized problem can be expressed through equation 2, but where the sensitivity matrix for the i^{th} datum given the j^{th} model cell is given by

$$\mathbf{G}_{ij} = \gamma \int_{\Delta V_j} \frac{z - z_i}{|\mathbf{r} - \mathbf{r}_i|^3} dv, \quad (8)$$

and is expressed through vector notation by Equation 6.

PRACTICAL ASPECTS

The inherent problem of non-uniqueness in gravity data is well-known. Processing of these data, for example, can be done via equivalent sources (Dampney, 1969) with no physical meaning carried to the sources. To combat this problem in 3D inversion a distance-based weighing is applied to the model to give equal probability for anomalous density within each model cell. The weighting, like the sensitivity, is a function of three-dimensional space.

Inversion of muon data is also confronted by non-uniqueness. The summation of densities creating a datum can occur anywhere along the corresponding ray path. An example would be an equivalent layer placed directly above the detectors to reproduce the data. The subsequent model would contain the same number of small, dense anomalies as the number of detectors, even though the data are caused by a single body.

Here we want to invert these data jointly. Our approach is to invert the gravity data with the usual distance weighting but not apply any special weighting to the muon data inversion.

JOINT METHODOLOGY

The linear inverse problem for each type of data can be formulated as a minimization of a global objective function subject to the data constraints for that type of data (Menke, 1989; Parker, 1994). This is achieved through Tikhonov formalism (Tikhonov and Arsenin, 1977). The optimal solution is found by minimizing a global objective function, □, which is comprised of the combination of a data misfit function, □$_d$, and model objective function, □$_m$:

$$\min\phi = \phi_d + \beta\phi_m\,, \quad (9)$$

and β is the trade-off parameter that finds the balance between model complexity and how well the recovered model reproduces the observed data. For muon data, Equation 9 becomes

$$\min\phi = \left\|\mathbf{W}_d(\mathbf{G}^{\mu}\Delta\boldsymbol{\rho} - \mathbf{d}^{\mu})\right\|^2 + \beta^{\mu}\left\|\mathbf{W}_m(\Delta\boldsymbol{\rho} - \boldsymbol{\rho}_o)\right\|^2, \quad (10)$$

where $\mathbf{W}_d$ is a diagonal matrix that normalizes the data by each standard deviation, σ_i, and $\boldsymbol{\rho}_o$ is a reference model. The model weighting matrix, $\mathbf{W}_m$, quantifies the smoothness of the model through volume-based derivatives. The depth or distance weighting function (Li and Oldenburg 2000) required for the gravity data can absorbed into the sensitivity matrix or model objective function. For clarity, this function is explicitly denoted by $\mathbf{W}$ in the model objective function. The minimization for the gravity data then becomes

$$\min\phi = \left\|\mathbf{W}_d(\mathbf{G}^{g}\Delta\boldsymbol{\rho} - \mathbf{d}^{g})\right\|^2 + \beta^{g}\left\|\mathbf{W}_m\mathbf{W}^{-1}(\Delta\boldsymbol{\rho} - \boldsymbol{\rho}_o)\right\|^2. \quad (11)$$

We now have two equations to solve for the density contrast $\Delta\rho$. The most straightforward result is the combination of Equations 10 and 11. However, there are two key aspects in combining these different data types. The first is that muon data often have very low signal-to-noise ratios (i.e. less than 2) and there are typically many more muon data than gravity data. A balance of discrepancies between both the number of data and quality of data needs to be achieved and thus the trade-off parameter, λ is used. The data misfit function for the joint inversion becomes

$$\phi_d = \left\|\mathbf{W}_d(\mathbf{G}^{g}\Delta\boldsymbol{\rho} - \mathbf{d}^{g})\right\|^2 + \lambda\left\|\mathbf{W}_d(\mathbf{G}^{\mu}\Delta\boldsymbol{\rho} - \mathbf{d}^{\mu})\right\|^2. \quad (12)$$

The second important point is the fact that the gravity data require a depth or distance weighting function whereas the muon data have equal probability to accrue density along each ray path and a weighting function is unnecessary. Therefore, the model objective function is

$$\phi_m = \beta\left(\left\|\mathbf{W}_m(\Delta\boldsymbol{\rho} - \boldsymbol{\rho}_o)\right\|^2 + \alpha\left\|\mathbf{W}_m\mathbf{W}^{-1}(\Delta\boldsymbol{\rho} - \boldsymbol{\rho}_o)\right\|^2\right), \quad (13)$$

where α is a trade-off between the depth-weighted and un-weighted density contrast. It should be noted that $\mathbf{W}_m$ is the same model weighting matrix. Substituting Equations 12 and 13 into 9, the minimization for the joint inversion is

$$\min\phi = \left\|\mathbf{W}_d(\mathbf{G}^{g}\Delta\boldsymbol{\rho} - \mathbf{d}^{g})\right\|^2 + \lambda\left\|\mathbf{W}_d(\mathbf{G}^{\mu}\Delta\boldsymbol{\rho} - \mathbf{d}^{\mu})\right\| + \beta\left(\left\|\mathbf{W}_m(\Delta\boldsymbol{\rho} - \boldsymbol{\rho}_o)\right\|^2 + \alpha\left\|\mathbf{W}_m\mathbf{W}^{-1}(\Delta\boldsymbol{\rho} - \boldsymbol{\rho}_o)\right\|^2\right). \quad (14)$$

The problem allows the freedom to balance the differing quantity and quality of the data types as well as incorporating the necessary depth weighting for the gravity data. We now move onto a synthetic example for illustration.

SYNTHETIC EXAMPLE

A synthetic example of a 3.17 g/cm^3 block at 150 m of depth representing a deposit in a 2.67 g/cm^3 half space is created. Eight muon detectors are placed in a "tunnel" underneath the block. To simulate field observations, muon ray-paths observations are binned at approximately every 5º in azimuth and 2º dip from 1º to 40º from vertical. These numbers translate to 81 and 17 azimuth and dip angles, respectively for a single detector. Figure 2 shows the ray paths of the muon data discretized to the mesh. Next, we assume we know the background density of 2.67 g/cm^3 and via Equation 5 calculate the anomalous data.

Five per cent Gaussian noise is then added to the anomalous signal of the 11,016 muon data. The simulated data are shown in Figure 3; it is typical to examine muon data through each detector as a function of angle. The dip, θ, is degrees from vertical. The azimuth, φ, is at 0º pointing the east. It should be noted that the effect from the block changes shape throughout the panels and is dependent upon the location of the deposit with respect to the sensor. The anomaly is located in the near-vertical angles throughout all azimuths in the third panel. The true anomalous density is presented in Figure 4a. The muon data are inverted (Figure 4b). Densities reach the same order of magnitude as the true anomalous density, but structurally they stretch to the surface. The non-uniqueness is exemplified by the "tails" reaching the detector locations to allow fit of the data.

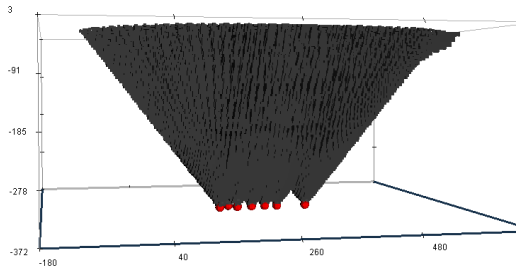

Figure 2. Muon ray paths that intersect the detectors (red spheres) are discretized into prismatic cells. The prisms with non-zero sensitivities for the 11000 muon ray paths are shown.

Anomalous gravity data are simulated at the surface on a grid of approximately 30 m. Five percent Gaussian noise has been added to the 625 data. In this case, the data values from the block are very small, on the order of tens of microgals. Anomalies with this magnitude are at the limit of detectability unless a carefully planned micro-gravity survey was carried out. Nevertheless, these data are inverted and the recovered model is shown in Figure 4c. The shape of the anomaly is spherical and centred close to the centre of mass of the true anomalous density. The maximum recovered density contrast is approximately 0.03 g/cm^3; much less than the true anomalous density. The recovered smooth, low amplitude model is a common result in this type of inversion.

Joint inversion of both data sets is performed. The number of muon data influences the model by constraining the result laterally and recovering larger anomalous densities as shown in Figure 4d. The colour scale is the same as the gravity inversion. Though the gravity data are small in magnitude, they still provide valuable information. The gravity data forces the model deeper to reproduce the simulated data. Overall, positive qualities of both methods have been brought out. The combination of the two types of data has increased the accuracy and resolution of the recovered models as compared to either method alone. Recovered density contrasts are within the same order of magnitude as the anomalous values. This anomalous density can be added to the background to yield a final density distribution.

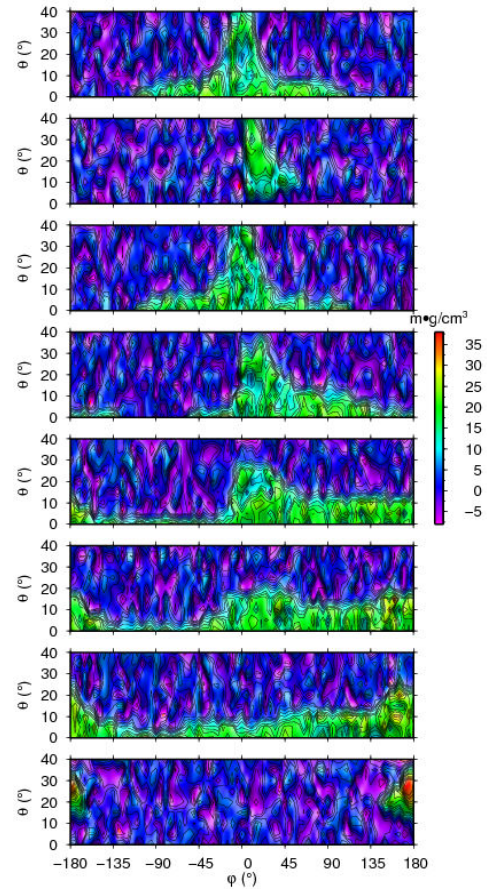

Figure 3. Anomalous muon data from the west-most receiver (top) to the east-most receiver (bottom).

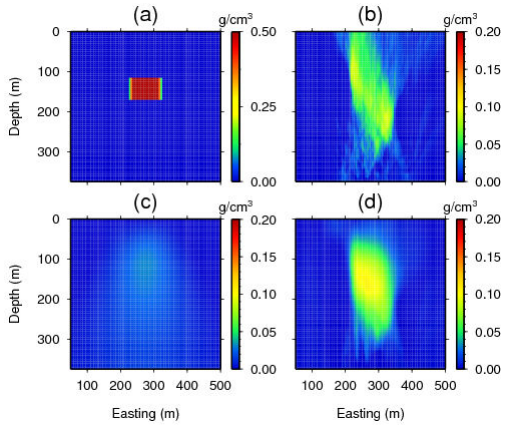

Figure 4: A slice of the true model (a) with a density contrast of 0.5 g/cm^3. The recovered models from the inversion of (b) muon, (c) gravity and (d) joint gravity and muon tomography are on the same colour scale.

CONCLUSIONS

Muon tomography is a new survey for mineral exploration. Here we have outlined the basic method of the survey and developed an inversion algorithm. As with any geophysical technique, additional information can greatly reduce the inherent non-uniqueness and we illustrate this by jointly inverting the muon data with conventional gravity data. The two data sets provide complementary information. A synthetic example illustrates the different types of data and sets the stage for joint inversions of field data.

REFERENCES

Alvarez, L. W., J. A. Anderson, F. E. Bedwci, J. Burhard, A. Fakhry, A. Girgis, F. Hassan, D. Iverson, G. Lynch, Z. Miligy, A. H. Moussa, M. Sharkawi, and L. Yazolino, 1970, Search for hidden chambers in the pyramids using cosmic rays: Science, 167, 832-839.

Blakely, R., 1996, Potential theory in gravity and magnetic applications: Cambridge University Press.

Bryman, D., 2011, Western Economic Diversification Canada press release, 17 March, online, http://www.aapsinc.com/wp-content/uploads/2011/03/WD-News-Release-AAPS-Technology-March-17-2011.pdf. Last accessed 31 Aug, 2011.

Dampney, C. N. G., 1969, The equivalent source technique: Geophysics, 34, 39-53.

Davis, K., D. W. Oldenburg, V. Kaminski, M. Pilkington, D. Bryman, J. Bueno, and Z. Liu, 2011, Joint 3D inversion of muon tomography and gravity data: Proceedings of the SEG International Workshop on Gravity, Electrical, and Magnetic Studies, Beijing, China.

Li, Y., and D. W. Oldenburg, 1998, 3-D inversion of gravity data: Geophysics, 63, 109-119.

Li, Y., and D. W. Oldenburg, 2000, Joint inversion of surface and three-component borehole magnetic data: Geophysics, 65, 540-552.

Menke, W. 1989, Geophysical data analysis: Discrete inverse theory: Academic Press.

Parker, R. L., 1994, Geophysical inverse theory: Princeton University Press.

Priedhorsky, W. C., K. N. Borozdin, G. E. Hogan, C. Morris, A. Saunders, L. J. Schultz, and M. E. Teasdale, 2003, Detection of high-z objects using multiple scattering of cosmic ray muons: Review of science instruments, 74, 4294-4298.

Reynolds, J. M., 1997, An introduction to applied and environmental geophysics: John Wiley & Sons, Ltd.

Schultz, L. J., K. N. Borozdin, J. J. Gomez, G. E. Hogan, J. A. McGill, C. L. Morris, W. C. Priedhorsky, A. Saunders, and M. E. Teasdale, 2004, Image reconstruction and material Z discrimination via cosmic ray muon radiography: Nuclear instruments and methods in physics research, Section A, accelerators, spectrometers, detectros, and associated equipment, 519, 678-694.

Tanaka, H. K. M., H. Taira, T. Uchida, M. Tanaka, M. Takeo, T. Ohminato, Y. Aoki, R. Nishitama, D. Shoji, and H. Tsuiji, 2010, Three-dimensional computational axial tomography scan of a volcano with cosmic ray muon radiography: Journal of Geophysical Research, 115, B12332.

Wang, G., L. J. Schultz, and J. Qi, 2009, Bayesian image reconstruction for imprving detection performance of muon tomography: IEEE transactions on image processing, 18, 1080-1089.